

Theoretical Investigation of Titanium Carbide, TiC: $X^3\Sigma^+$, $a^1\Sigma^+$, $A^3\Delta$, and $b^1\Delta$ States

Apostolos Kalemios and Aristides Mavridis*

Laboratory of Physical Chemistry, Department of Chemistry, National and Kapodistrian University of Athens, PO Box 64 004, 157 10 Zografou, Athens, Greece

Received: November 9, 2001; In Final Form: February 1, 2002

Four states, $1,^3\Sigma^+$ and $1,^3\Delta$, have been investigated by ab initio multireference methods coupled with quantitative basis sets. The ground state is, formally, of $^3\Sigma^+$ symmetry with $D_e = 82.34$ kcal/mol, $r_e = 1.712$ Å, and with the $^1\Sigma^+$ state just 1.55 kcal/mol above the X-state.

Introduction

The present work reports accurate multireference variational calculations on the ground and three excited states of the TiC carbide. As in all first-row transition metal carbides M–C, M = Sc ($Z = 21$) to Cu ($Z = 29$), the literature, either experimental or theoretical, is rather limited.¹ Recently, we have investigated the ScC² and FeC³ systems, as well as the series of the cationic carbides ScC⁺, TiC⁺,⁴ and VC⁺, CrC⁺.⁵ For the TiC diatomic Bauschlicher and Siegbahn in 1984⁶ reported close to equilibrium multireference (MRCI) calculations on four states ($^3\Sigma^+$, $^1\Sigma^+$, $^3\Delta$, and $^3\Pi$), while in 1996 Hack et al.⁷ calculated the $^3\Sigma^+$ and $^1\Sigma^+$ states using density functional (DFT), coupled cluster (CCSD(T)), and MRCI techniques. Also, very recently the $^3\Sigma^+$ and $^1\Sigma^+$ states of TiC have been examined by fixed node diffusion quantum Monte Carlo methods.⁸ Computational details and results obtained from refs 6–8 are summarized in Table 1.

From Table 1 we observe that at the MRCI level^{6,7} the ground state is predicted to be of $^3\Sigma^+$ symmetry (which is rather correct but see below), with the first excited $^1\Sigma^+$ state 3.03⁶ or 3.58⁷ kcal/mol higher. We also observe that while D_e values at the MRCI and CCSD(T) levels are more or less similar, DFT (LSDA, B3LYP, and BPW91) predictions are in striking disagreement among themselves and with ab initio findings. As a matter of fact the LSDA and BPW91 functionals predict the wrong ordering, i.e., the $^1\Sigma^+$ as the ground state of TiC. The Monte Carlo approach gives a 12 kcal/mol larger D_e value than the D_e values of the MRCI methods, and a rather too large (12.5 kcal/mol) $^1\Sigma^+ \leftarrow ^3\Sigma^+$ energy separation.⁸

With the purpose of obtaining quantitative binding energies, to confirm that the $^3\Sigma^+$ is indeed the ground state, to accurately locate the first excited state, and to comprehend the Ti–C bonding, we have constructed potential energy curves (PEC) for the $^3\Sigma^+$, $^1\Sigma^+$, $^3\Delta$, and $^1\Delta$ states, employing large basis sets and CASSCF + single + double replacements (=MRCI) methods. In particular, for the Ti atom we have used the ANO basis set of Bauschlicher,¹⁰ 21s16p9d6f4g, and for the C atom the cc-pVQZ correlation consistent basis set of Dunning,¹¹ both generally contracted to [7s6p4d3f2g/Ti;5s4p3d2f1g/C]. Our CASSCF space is composed of the $4s + 4p + 3d(-3d_z^2) = 8$ orbitals on Ti, and, the $2s + 2p = 4$ orbitals on the C atom, a total of 12 functions. Considering the $1s^2(\text{C})$ and the $1s^2 2s^2 2p^6 3s^2 3p^6$ (Ti) as core electrons, our zeroth-order space was constructed by distributing the 4+4 valence electrons to 12 orbitals, enforcing at the same time symmetry and equivalence conditions. Valence “dynamical” correlation was obtained by

single+double excitations out of the reference space (CASSCF + 1 + 2 = MRCI) at the internally contracted MRCI level. The size of the MRCI expansions ranges from 2×10^6 ($a^1\Sigma^+$, $b^1\Delta$) to 3×10^6 ($X^3\Sigma^+$, $A^3\Delta$) configurations, and the size extensivity error is 1.4(0.5) mhartree at the MRCI(+Davidson correction) level.

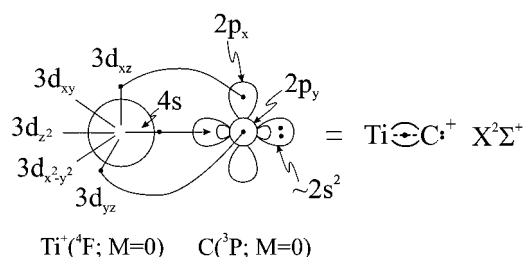
For the four states examined we report full potential energy curves (PEC), dissociation energies (D_e), spectroscopic parameters (r_e and ω_e), and dipole moments (μ).

All our calculations were performed with the MOLPRO 2000.1 suite.¹²

Results and Discussion

At the MRCI level, the atomic energy separations $\text{Ti}(a^5F \leftarrow a^3F, b^3F \leftarrow a^3F)$ are 0.958 and 1.556 eV, respectively, in acceptable agreement with the experimental values of 0.806 and 1.420 eV.¹³ These separations are of interest to the present work due to their implicit participation in the bonding process (vide infra). Table 2 reports all our numerical results and Figure 1 shows the four potential energy curves at the MRCI level.

Now, the ground state of the TiC^+ cation is of $2\Sigma^+(\sim 1\sigma^2 2\sigma^1 1\pi_x^2 1\pi_y^2)$, counting active electrons only) symmetry, portrayed in the following valence-bond-Lewis (vbl) picture,



suggesting two π and $1/2\sigma$ bonds, with $D_e = 86.4(88)$ kcal/mol and $r_e = 1.696(1.70)$ Å at the MRCI(+Q) level (ref 4). Given the above scheme, one could surmise on the low-lying states of the neutral TiC species. Clearly, by adding a single electron to a $3d_\delta$ or $3d_\sigma$ orbital of the TiC^+ , the TiC states of $1,^3\Delta$ or $1,^3\Sigma^+$ symmetry are realized, respectively. In addition, due to the passive character of the $3d_\delta$ or $3d_\sigma$ added electron, it is anticipated that the bonding features of TiC will be very similar to those of TiC^+ . Indeed, our numerical findings are in keeping with the above discussion: the states $^3\Sigma^+$ and $^1\Sigma^+$ are essentially degenerate within the accuracy of our methods, with the $^3\Sigma^+$

TABLE 1: Previous Theoretical Results on TiC^a

state	method	$-E$	D_e	r_e	ω_e	μ	T_e
Reference 6							
$^3\Sigma^+$	CASSCF ^b	74.26	1.76	860			0.0
	MRCI ^c	69.64	1.75	850	1.53		0.0
	MRCI+Q ^d	71.03	1.77	830			0.0
Reference 7							
	ROHF	886.029 59	-28.60	1.617	1088	2.90	0.0
	CASSCF ^e	886.213 16	54.19	1.723	702	2.39	0.0
	MRCI ^f	886.297 00	65.03	1.733	704	2.73	0.0
	CCSD ^g	886.477 83	55.35	1.682	768		
	CCSD(T) ^g	886.508 05	70.34	1.703	805		
	LSDA	885.538 50	139.75	1.657	997	3.03	5.56
	B3LYP	887.359 74	83.02	1.668	988	3.16	0.0
	BPW91	887.420 00	110.46	1.679	972	3.02	1.55
Reference 8							
	FNDQMC ^h	81.2	1.70				0.0
Reference 9							
	exptl ⁱ	105 ± 6					
Reference 6							
$^1\Sigma^+$	CASSCF ^b	73.23	1.81	700			1.23
	MRCI ^c	66.61	1.80	830	2.82		3.03
	MRCI+Q ^d	68.80	1.79	830			2.23
Reference 7							
	ROHF	886.007 84	-42.20	1.539	1242	7.91	13.65
	CASSCF ^e	886.211 15	52.81	1.784	579	1.74	1.26
	MRCI ^f	886.291 29	61.34	1.790	592	2.16	3.58
	LSDA	885.547 34	145.28	1.602	994	6.41	0.0
	B3LYP	887.357 25	81.47	1.604	980	6.63	1.56
	BPW91	887.422 36	111.85	1.641	924	5.79	0.0
Reference 8							
	FNDQMC ^h	68.7	1.82				12.5
Reference 6							
$^3\Delta$	CASSCF ^b	46.38	1.80	880			27.88
	MRCI ^c	50.14	1.79	860	7.78		19.50
	MRCI+Q ^d	50.96	1.80	880			20.07
$^3\Pi$	CASSCF ^b	27.83	1.76	840			46.43
	MRCI ^c	23.81	1.76	830	3.86		45.83
	MRCI+Q ^d	24.80	1.77	830			46.23

^a Energies E (hartree), dissociation energies D_e (kcal/mol), bond lengths r_e (Å), harmonic frequencies ω_e (cm⁻¹), dipole moments μ (debye), and energy separations T_e (kcal/mol). ^b Complete active space SCF of 8 active electrons in 10 orbitals, [5s4p3d1f/ti 3s3p1d/c] basis. ^c Externally contracted CI out of the most important CAS configuration functions. ^d MRCI+multireference Davidson correction. ^e Reference space as in b, [10s8p3d/ti 4s2p1d/c] basis. ^f CI out of CAS configurations with coefficients greater than 0.02. ^g Although it is not explicitly said, we believe that at least the 3s²3p⁶ "core" electrons of Ti have been included in the CC-calculations. ^h Fixed node diffusion quantum Monte Carlo with effective core potentials for both C and Ti. ⁱ $D_e = D_0 + \omega_e/2 = 432 \pm 25$ kJ/mol + 1126/2 cm⁻¹, a maximum D_e value is obtained by Knudsen effusion mass spectrometric methods; ω_e of unknown origin.

being *nominally* the ground state, followed by the $^3\Delta$ and $^1\Delta$ states (vide infra).

$X^3\Sigma^+$. The leading CASSCF equilibrium configuration is $|X^3\Sigma^+\rangle \sim 0.91|1\sigma^2 2\sigma^1 3\sigma^1 1\pi_x^2 1\pi_y^2\rangle$, correlating to Ti($a^3F; M=0$) + C($^3P; M=0$) fragments, Figure 1. The equilibrium CASSCF atomic populations are (Ti/C)

$$4s^{0.80} 3d_{z^2}^{0.58} 4p_z^{0.23} 4p_x^{0.05} 4p_y^{0.05} 3d_{xz}^{0.95} 3d_{yz}^{0.95} 4f^{0.03} / \\ 2s^{1.72} 2p_z^{0.64} 2p_x^{0.98} 2p_y^{0.98} 3d^{0.06}$$

with corresponding populations at infinity

Ti($a^3F; M=0$):

$$4s^{1.83} 4p_z^{0.05} 4p_x^{0.06} 4p_y^{0.06} 3d_{xz}^{0.83} 3d_{yz}^{0.83} 3d_{x^2-y^2}^{0.17} 3d_{xy}^{0.17}$$

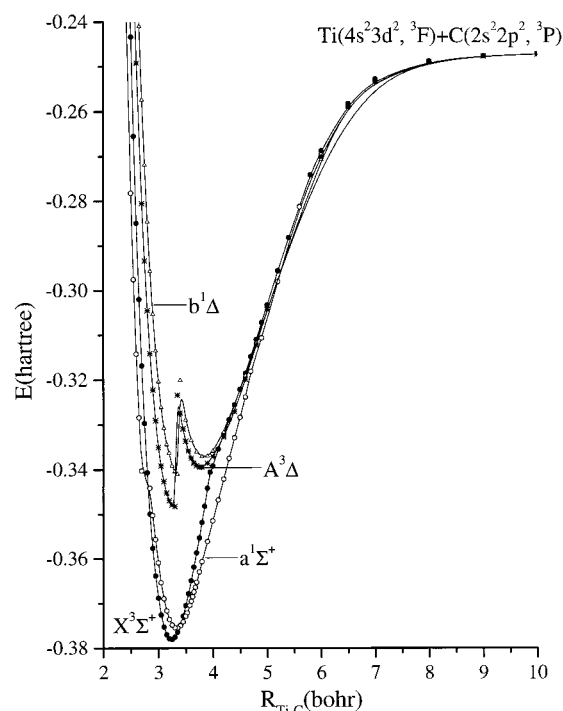
$$C(^3P; M=0): 2s^{1.95} 2p_z^{0.05} 2p_x^{1.0} 2p_y^{1.0}$$

Contrasting the above distributions the formation of two π bonds

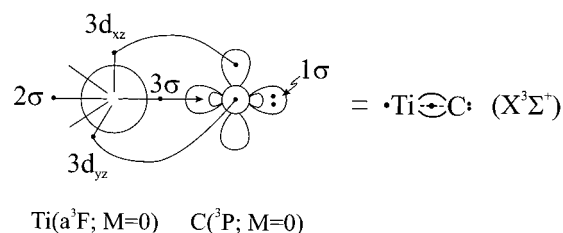
TABLE 2: Absolute Energies E (hartree), Dissociation Energies D_e (kcal/mol), Bond Lengths r_e (Å), Harmonic Frequencies ω_e (cm⁻¹), Dipole Moments μ (debye), and Energy Separations T_e (kcal/mol) of the $X^3\Sigma^+$, $a^1\Sigma^+$, $A^3\Delta$, and $b^1\Delta$ TiC States

state ^a	method ^b	$-E$	D_e	r_e	ω_e	μ	T_e
$X^3\Sigma^+$	MRCI	886.378 07	82.34	1.712	869	2.61	0.0
	MRCI+Q	886.384 7	83.2	1.716	861		0.0
$a^1\Sigma^+$	MRCI	886.375 60	80.80	1.761	756	2.33	1.55
	MRCI+Q	886.382 0	81.5	1.765	748		1.7
$A^3\Delta_G$	MRCI	886.348 15	64.10	1.75		7.43	18.78
	MRCI+Q	886.355 8	65.48	1.75			18.1
$A^3\Delta_L$	MRCI	886.339 40	58.61	1.993	572	2.87	
	MRCI+Q	886.346 4	59.6	1.992	590		
$b^1\Delta_G$	MRCI	886.340 36	59.21	1.77		7.13	23.66
	MRCI+Q	886.349 2	61.3	1.77			
$b^1\Delta_L$	MRCI	886.337 16	57.20	2.030	562	2.84	
	MRCI+Q	886.343 8	57.9	2.030	551		

^a G and L refer to global and local minima, respectively. ^b +Q refers to the Davidson correction.

**Figure 1.** Potential energy curves of the TiC $X^3\Sigma^+$, $a^1\Sigma^+$, $A^3\Delta$, and $b^1\Delta$ states at the MRCI level. Energies have been shifted by +886.0 hartree.

is obvious, while a half σ bond is created due to a transfer of $\sim 0.4 e^-$ from the Ti 4s^{1.83} electrons to the almost empty 2p_z C orbital. Notice the complete removal of the 3d_{x²-y²}, 3d_{xy} orbitals upon bonding, clearly described by the following icon with



$1\sigma \sim 0.92(2s)$, $2\sigma \sim 0.65(4s) - 0.18(2s) - 0.41(4p_z)$, and $3\sigma \sim 0.58(3d_{z^2}) - 0.75(2p_z)$. The above description is in agreement with the conclusions of Bauschlicher and Siegbahn.⁶ However, our D_e value is larger by 12 kcal/mol, our bond distance r_e

shorter by 0.04 Å, and our dipole moment μ larger by 1.1 D than those of ref 6. We attribute these significant numerical differences to the smaller basis sets, and, perhaps, to the truncated zeroth order space of these workers. As was expected the $D_e = 86.4(88.0)$ kcal/mol, $r_e = 1.696(1.70)$ Å, and $\omega_e = 859(847)$ cm^{-1} values of the $\text{TiC}^+(\text{X}^3\Sigma^+)$ at the MRCI(+Q) level,⁴ are very similar to the corresponding values of $\text{TiC}(\text{X}^3\Sigma^+)$ at the same level of theory, namely, $D_e = 82.3(83.2)$ kcal/mol, $r_e = 1.712(1.716)$ Å, and $\omega_e = 869(861)$ cm^{-1} , Table 2. Experimentally, an upper limit $D_e = 105 \pm 6$ kcal/mol value is reported in the literature obtained by Knudsen effusion mass spectrometry.⁹ By using the results of TiC^+ (ref 4) the ionization energy (IE) of TiC is obtained, $\text{IE} = 6.49$ eV.

$\text{a}^1\Sigma^+$. From Table 2 and Figure 1 it is clear that the $\text{X}^3\Sigma^+$ and $\text{a}^1\Sigma^+$ states are almost degenerate within our methods, the $\text{a}^1\Sigma^+ \leftarrow \text{X}^3\Sigma^+$ difference being 1.55(1.71) kcal/mol at the MRCI(+Q) level. By extracting more valence correlation and/or by adding core-correlation effects it is understandable that the ordering of the two states could even be inverted at the nonrelativistic level of theory. The corresponding energy gap obtained by Bauschlicher and Siegbahn⁶ is twice as large, indicating again the effect of the one electron basis set.

The $\text{a}^1\Sigma^+$ state traces its lineage to $\text{Ti}(\text{a}^3\text{F}; M=0) + \text{C}(\text{P}; M=0)$ described at equilibrium by two leading CASSCF configurations,

$$|\text{a}^1\Sigma^+\rangle \sim 0.78|1\sigma^2 2\sigma^2 1\pi_x^2 1\pi_y^2\rangle - 0.44|1\sigma^2 3\sigma^2 1\pi_x^2 1\pi_y^2\rangle$$

The CASSCF atomic Mulliken populations (Ti/C),

$$4s^{0.63} 3d_{z^2}^{0.36} 4p_z^{0.41} 4p_x^{0.04} 4p_y^{0.04} 3d_{xz}^{1.02} 3d_{yz}^{1.02} 4f^{0.03}/ \\ 2s^{1.72} 2p_z^{0.85} 2p_x^{0.91} 2p_y^{0.91} 3d^{0.06}$$

in conjunction with the atomic populations at infinity (see state $\text{X}^3\Sigma^+$), indicate the formation of two π bonds and a σ interaction caused by the transfer of about 0.5 e^- from the $4s3d_{z^2}4p_z$ hybrid on Ti to the empty $2p_z$ C orbital. However, the presence of the $|1\sigma^2 3\sigma^2 1\pi_x^2 1\pi_y^2\rangle$ configuration with a relatively large coefficient diminishes the bonding ability of the 2σ orbital. This is also corroborated by the fact that the D_e value of the present state is practically the same to the binding energy of the $\text{X}^3\Sigma^+$ state which carries a $1/2 \sigma$ bond, that is the "0.44" configuration, somehow, partially cancels the "0.78" one. The D_e and r_e values obtained at the MRCI(+Q) level are 80.8(81.5) kcal/mol and 1.761(1.765) Å, as compared to 66.6(68.8) kcal/mol and 1.80-(1.79) Å, respectively, of Bauschlicher and Siegbahn,⁶ Tables 1 and 2.

By examining Table 1, it is proper to say at this point that the density functional approach for both states, $\text{X}^3\Sigma^+$ and $\text{a}^1\Sigma^+$ (ref 7), fails.

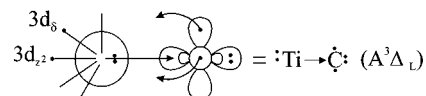
$\text{A}^3\Delta$. The PEC of Figure 1 displays two minima, a local (L) and a global (G) one at 3.75 and 3.30 bohr, respectively. The leading MRCI configurations and atomic Mulliken distributions at the L and G minima are

$$|\text{A}^3\Delta_L\rangle \sim \\ |1\sigma^2 2\sigma^2 3\sigma^1 (0.62 1\bar{\pi}_x^1 1\pi_y^1 1\delta_-^1 - 0.44 1\pi_x^1 1\pi_y^1 1\bar{\delta}_-^1 + \\ 0.36 1\pi_x^1 1\bar{\pi}_y^1 1\delta_-^1)\rangle \\ 4s^{0.83} 3d_{z^2}^{0.97} 4p_z^{0.34} 4p_x^{0.05} 4p_y^{0.05} 3d_{xz}^{0.17} 3d_{yz}^{0.17} 3d_{xy}^{1.0} 4f^{0.04}/ \\ 2s^{1.74} 2p_z^{1.05} 2p_x^{0.77} 2p_y^{0.77} 3d^{0.06}$$

and

$$|\text{A}^3\Delta_G\rangle \sim \\ |1\sigma^2 2\sigma^1 (0.89 1\pi_x^2 1\pi_y^2 - 0.13 2\pi_x^2 1\pi_y^2 - \\ 0.13 1\pi_x^2 2\pi_y^2) 1\delta_-^1\rangle \\ 4s^{0.14} 3d_{z^2}^{0.46} 4p_z^{0.13} 4p_x^{0.07} 4p_y^{0.07} 3d_{xz}^{0.84} 3d_{yz}^{0.84} 3d_{xy}^{1.0} 4f^{0.03}/ \\ 2s^{1.62} 2p_z^{0.62} 2p_x^{1.05} 2p_y^{1.05} 3d^{0.06}.$$

The $\text{A}^3\Delta_L$ state correlates to $\text{Ti}(\text{a}^3\text{F}; M=\pm 2) + \text{C}(\text{P}; M=0)$ atomic states. The populations in conjunction with the leading configurations clearly support the following bonding picture imply-



ing a σ bond due to the migration of 0.7 e^- from the Ti $4s^2$ orbital to the $2p_z$ C atom, while through the π frame $\sim 0.4 e^-$ are moving from the C to the d_{xz} , d_{yz} empty orbitals of the Ti atom, causing a slight π interaction. Overall 0.4 e^- are moving from Ti to the C atom. With respect to the asymptotic products, $D_e(\text{L}) = 58.6$ kcal/mol at $r_e(\text{L}) = 1.993$ Å. Moving now toward the G-minimum a complete reorganization of the electronic structure takes place due to a severe avoided crossing with a higher $^3\Delta$ state originating from a Ti $\text{a}^5\text{F}(4s^1 3d^3)$ state, 0.806 eV above the a^3F state. Despite our efforts it was not possible to avoid the sharp drop of the PEC around the G-minimum. The bonding icon is similar to that of the $\text{X}^3\Sigma^+$ state but with the 2σ electron moved to a $3d_\delta$ orbital, therefore the two atoms form two π and a $1/2\sigma$ bonds. With respect to $\text{Ti}(\text{a}^5\text{F}) + \text{C}(\text{P})$ the binding energy is $64.1 + \Delta E(\text{a}^5\text{F} \leftarrow \text{a}^3\text{F}) = 82.7$ kcal/mol at $r_e = 1.75$ Å, using the experimental $\text{a}^5\text{F} \leftarrow \text{a}^3\text{F}$ gap, practically the same with the corresponding values of the $\text{X}^3\Sigma^+$ state. The diabatic origin of the $\text{A}^3\Delta_G$ state rationalizes the fact that this state is 18.8 kcal/mol above the $\text{X}^3\Sigma^+$ and not degenerate, or even lower in energy than the $\text{X}^3\Sigma^+$ state.

$\text{b}^1\Delta$. This is the singlet analogue of the previously discussed $\text{A}^3\Delta$ state; it correlates to $\text{Ti}(\text{a}^3\text{F}; M=\pm 2) + \text{C}(\text{P}; M=0)$ and its PEC presents two minima, a local (L) and a global (G), at the same internuclear distances as in the $\text{A}^3\Delta$ state, Figure 1. Also, the leading configurations and Mulliken densities differ only slightly from those of the $\text{A}^3\Delta$ state, therefore both states share the same bonding description. The L-minimum occurs at 2.030 Å, 0.04 Å larger than the corresponding $\text{A}^3\Delta_L$ minimum, stems directly from the end products, and lies just 1.38 kcal/mol above the $\text{A}^3\Delta_L$ state, Figure 1. Moving toward the G-minimum a severe avoided crossing occurs around 1.77 Å creating similar morphological features as in the $\text{A}^3\Delta_G$ PEC, Figure 1, but correlating to $\text{Ti } \text{b}^3\text{F}(4s^1 3d^3) + \text{C}(\text{P})$. With respect to the $\text{Ti}(\text{b}^3\text{F}) + \text{C}(\text{P})$ fragments the binding energy (internal bond strength) obtained is, $59.2 + \Delta E(\text{b}^3\text{F} \leftarrow \text{a}^3\text{F}) = 91.9$ kcal/mol using the experimental ΔE gap. Naturally, the bonding features of the $\text{b}^1\Delta_G$ state are identical to those of the $\text{A}^3\Delta_G$, with the former state being 4.9 kcal/mol above the latter. Finally, we would like to observe the very large differences between the $^{1,3}\Delta_G$ and $^{1,3}\Delta_L$ dipole moments, $\Delta\mu \approx 4$ D.

Final Remarks

The $^{1,3}\Sigma^+$ and $^{1,3}\Delta$ states of the TiC system were examined by CASSCF+1+2 methods and quantitative basis sets. Somehow in line with Hund's rules the $^3|\Lambda|$ states are lower in energy

than the corresponding $^1|\Lambda|$ ones, albeit by only 1.55 ($a^1\Sigma^+ \leftarrow X^3\Sigma^+$) and 1.38 ($b^1\Delta_L \leftarrow A^3\Delta_L$) kcal/mol. Formally, the X-state is of $^3\Sigma^+$ symmetry with $D_e = 82.34(83.2)$ kcal/mol at the MRCI(+Q) level, contrasted to an upper limit experimental value of 105 ± 6 kcal/mol. Our previous experience with similar systems and the MRCI approach, suggest that the experimental D_e value is rather overestimated. For the present system, further increase of the basis set, inclusion of core-valence correlation and scalar relativistic effects, does not seem to affect the binding energy significantly. The electronic structure of these four states can be rationalized by grafting a σ or δ "observer" electron to the $\text{TiC}^+ X^2\Sigma^+$ state without perturbing seriously the bonding characteristics of TiC^+ , as reflected on the D_e and r_e values of TiC . In all states the bonding can be attributed to a $1/2 \sigma, \pi_x, \pi_y$ interaction, with the observer electron defining the symmetry of each state. The formation of two π and a half σ bonds forces the C atom in a $M=0$ configuration ($2p_x^1 2p_y^1$), with the empty $2p_z$ orbital acquiring electron density originating from the Ti $4s^2$ or $4s^1 3d^3$ configurations.

References and Notes

- (1) For instance, see: Harrison, J. F. *Chem. Rev.* **2000**, *100*, 679 and references therein.
- (2) Kalemos, A.; Mavridis, A.; Harrison, J. F. *J. Phys. Chem. A* **2001**, *105*, 755.
- (3) Tzeli, D.; Mavridis, A. *J. Chem. Phys.* In press.
- (4) Kerkines, I. S. K.; Mavridis, A. *J. Phys. Chem. A* **2000**, *104*, 11777.
- (5) Kerkines, I. S. K.; Mavridis, A. Manuscript in preparation.
- (6) Bauschlicher, C. W., Jr.; Siegbahn, P. E. M. *Chem. Phys. Lett.* **1984**, *104*, 331.
- (7) Hack, M. D.; Maclagan, R. G. A. R.; Scuseria, G. E.; Gordon, M. S. *J. Chem. Phys.* **1996**, *104*, 6628.
- (8) Sokolova, S.; Lüchow, A. *Chem. Phys. Lett.* **2000**, *320*, 421.
- (9) Kohl, F. J.; Stearns, C. A. *High Temp. Sci.* **1974**, *6*, 284.
- (10) Bauschlicher, C. W., Jr. *Theor. Chim. Acta* **1995**, *92*, 83.
- (11) Dunning, T. H., Jr. *J. Chem. Phys.* **1989**, *90*, 1007.
- (12) MOLPRO is a package of ab initio programs written by H.-J. Werner and P. J. Knowles, with contributions from R. D. Amos, A. Bernhardsson, A. Berning, P. Celani, D. L. Cooper, M. J. O. Deegan, A. J. Dobbyn, F. Eckert, C. Hampel, G. Hetzer, T. Korona, R. Lindh, A. W. Lloyd, S. J. McNicholas, F. R. Manby, W. Meyer, M. E. Mura, A. Nicklass, P. Palmieri, R. Pitzer, G. Rauhut, M. Schütz, H. Stoll, A. J. Stone, R. Tarroni, and T. Thorsteinsson.
- (13) Moore, C. E. Atomic Energy Levels. NSRDS-NBS Circular No. 35; U. S. Government Printing Office: Washington, DC, 1971.